Ferricrete Classification, Morphology, Distribution, and Carbon-14 Age Constraints

By Philip L. Verplanck, Douglas B. Yager, Stanley E. Church, and Mark R. Stanton

Chapter E15 of
Integrated Investigations of Environmental Effects of Historical Mining in the Animas River Watershed, San Juan County, Colorado
Edited by Stanley E. Church, Paul von Guerard, and Susan E. Finger

Professional Paper 1651

U.S. Department of the Interior
U.S. Geological Survey

Contents

Figures

Tables

Chapter E15
Ferricrete Classification, Morphology, Distribution, and Carbon-14 Age Constraints

By Philip L. Verplanck, Douglas B. Yager, Stanley E. Church, and Mark R. Stanton

Abstract

As part of the U.S. Geological Survey Abandoned Mine Lands Initiative Animas River watershed investigation, we mapped the distribution and characterized the physical properties of ferricrete deposits to build a framework for determining the processes responsible for their formation and preservation. Ferricretes are stratified iron oxyhydroxide deposits, or clastic sedimentary deposits cemented by stratified iron oxyhydroxide. Three classes of ferricrete were distinguished and mapped: those that contained essentially no clasts (spring and bog iron deposits), those that contained predominantly angular clasts, most commonly monolithologic (iron-cemented colluvial deposits), and those that contained subangular to rounded clasts of several lithologies (iron-cemented alluvial deposits). In addition, deposits that have a black matrix were mapped as manganocrete.

To characterize the deposits, the mineralogy and chemistry of ferricrete matrix were determined. Organic material from 71 samples was analyzed by the ^{14}C dating technique to evaluate the temporal distribution. These ages range from 9,150±50 years B.P. to modern; most ages fall between 5,000 years B.P. and the present.

Ferricrete deposits are not evenly distributed within the study area but crop out in conjunction with specific geologic and geomorphologic features. Ferricrete and manganocrete commonly form in surficial deposits on or down gradient from sulfide-rich bedrock, fractures, or veins. Most ferricrete deposits are found within or down gradient from parts of the watershed where hydrothermal alteration was most intense. Manganocrete deposits crop out primarily along the Animas River and its tributaries upstream of the town of Eureka. Polymetallic veins in this portion of the watershed contain abundant manganese minerals which, when oxidized, result in manganese mobilization.

Introduction

Ferricretes are present in many mining districts. They have been used as exploration guides and as indicators of paleo-weathering conditions. However, no systematic investigations of their morphology and distribution within a watershed have been published. As part of the U.S. Geological Survey (USGS) Abandoned Mine Lands Initiative Animas River watershed investigation, we mapped the distribution and characterized the physical properties of ferricrete deposits to build a framework for determining the processes responsible for their formation and preservation. The Animas River watershed study area is ideally suited for a detailed study of ferricretes because of the presence of numerous ferricrete outcrops, an abundance of iron-rich springs, a wide variety of alteration types, rugged terrain with deeply incised valleys, and relatively thin vegetative cover. The deeply incised valleys and relatively thin vegetative cover provide an opportunity to view many sections where ferricrete deposits are located. Thus, the setting provides the opportunity to conduct a multidisciplinary study of the distribution of ferricrete in both time and space and to evaluate the processes responsible for the formation of ferricrete deposits.

Purpose and Scope

The objectives of this study are:

- To present a descriptive classification for ferricrete deposits within the Animas River watershed study area on the basis of clast type, degree of rounding, distribution, and morphology. Physical parameters (on the basis of field measurements), mineralogy, chemistry, and geochronology were determined from many localities within the watershed. This classification scheme was also used to produce a map of the ferricrete distribution (Yager and Bove, this volume, Chapter E1, pl. 2).

- To evaluate the temporal and spatial distribution of ferricrete within the watershed throughout the late Pleistocene and Holocene.
- To provide the framework for the more detailed investigations on the geomorphologic, hydrologic, and geochemical processes controlling ferricrete formation (Vincent and others, this volume, Chapter E16; Wirt and others, this volume, Chapter E17).

Background

Initially, the term ferricrete was used to describe conglomerates that were cemented by iron oxides, analogous to the usage of the term calcrete (Lamplugh, 1902). Ferricrete has also been used to describe iron-rich soil zones that form by the replacement of argillaceous or sandy argillaceous matrix by iron oxyhydroxides (Mason and others, 1959; Nahon, 1991). Soil scientists have attempted to relate these relict paleo-weathering profiles to climatic variations (Battiau-Queney, 1996). In historical mining districts in the Rocky Mountain region and in Australia, the term ferricrete has been used to describe a wide range of iron oxyhydroxide-rich material including conglomerates, soils, and paleo-iron bog deposits. In addition, the terms ferrosinter and ferroconglomerate have been used to describe iron-rich spring and alluvial deposits (Kirkham and others, 1995). We adopt the definition from Furniss and Hinman (1998), which states that ferricretes are stratified iron oxyhydroxide deposits or clastic sedimentary deposits cemented by stratified iron oxyhydroxide.

Descriptions of iron-rich deposits date back to some of the earliest geologic investigations in the study area. Spring-type limonite deposits and iron-cemented alluvial deposits were observed along Cement and Mineral Creeks during the initial surveys of the geology and mineralized rocks of San Juan County (Comstock, 1883; Ransome, 1901). Figure 1 displays locations of most creeks, peaks, and towns referred to in this report. Geologists working in the San Juan Mountains of Colorado during the late 19th century described numerous iron-oxide deposits associated with iron bogs and springs along valley floors, as well as iron-cemented creek beds (Comstock, 1883; Cross and Purington, 1899; Ransome, 1901; Cross and others, 1905). Comstock (1883, p. 169) noted, “Large deposits of bog iron have been made along the banks, especially in portions of Cement and Mineral Creeks.” Comstock’s observations are direct evidence that ferricrete deposits and iron precipitates in Cement and Mineral Creeks were part of the local landscape prior to hard rock mining in the Silverton area. Ransome (1901) concluded from his studies in the district that as meteoric spring water came in contact with the atmosphere, the iron oxidized and accumulated near the spring to form bog iron deposits.

The first study of ferricrete in the western San Juan Mountains (Hanshaw, 1974) examined the bog iron deposit at the Iron Springs placer claim in Ophir Valley, a headwater subbasin adjacent to and west of Middle Fork Mineral Creek subbasin. This bog iron deposit is the largest known goethite deposit in Colorado. Approximately 91,000 metric tons of ore was mined for use as smelter flux and paint pigment (Cross and Purington, 1899; Harrer and Tesch, 1959). Vhay (1962, p. 247) surmised that the iron oxide in the Iron Springs deposit was likely “derived by the weathering of the pyrite disseminated through the large mass of hydrothermally altered rock that forms the whole mountain to the north of the valley.” Chemical analyses of different iron-bearing lithologies within the deposit had a range in iron concentration (as Fe_2O_3) from 58.8 to 73.8 weight percent. The samples also contained substantial concentrations of zinc ranging from 700 to 1,500 ppm, and lesser concentrations of copper ranging from 50 to 200 ppm and lead ranging from 15 to 50 ppm (Hanshaw, 1974).

A wood fragment located 1 m above the base of the deposit gave a radiocarbon age of 8,250 yr B.P. (Hanshaw, 1974). This sample was about 7.3 m from the top of the deposit, yielding an average accumulation rate of 0.9 mm/yr. Other wood fragments from different stratigraphic levels within the deposit yielded accumulation rates ranging from 0.6 to 1.6 mm/yr (Hanshaw, 1974).

Investigations to determine premining metal loading in historical mining districts have tried to utilize ferricrete deposits as proxies for paleo-weathering conditions (Plumlee and others, 1995; Logsdon and others, 1996; Furniss and others, 1999; Miller and others, 1999). At the Summitville mine, Plumlee and others (1995) used aerial photographs taken prior to open-pit mining to map ferricretes formed by natural springs. The ferric oxide minerals that formed the ferricretes were precipitated by acidic, iron-rich ground water as it flowed from springs and were interpreted to delineate the locations of naturally acidic springs that flowed prior to mining (Plumlee and others, 1995). The authors noted that ferricrete deposits tended to follow major structural features or were located along contacts between lithologies with differing hydrologic characteristics.

Furniss and others (1999) dated and analyzed ferricretes at the New World mining district of south-central Montana, concluding that the ferricretes are evidence that discharge of acidic, metal-bearing water predated mining activity. Twenty-two radiocarbon dates on wood fragments in the ferricrete deposits, ancient stream terraces and aprons around natural springs, ranged from 8,840±50 yr B.P. to the present. Chemical compositions of modern and ancient iron oxyhydroxides were compared at specific sites to gain insight into premining conditions. Furniss and Hinman (1998) concluded that within the New World mining district, similar chemical conditions exist today in natural iron-rich springs as have existed since the exposure of the sulfide-rich mineral deposit.

More recently, preliminary mapping of ferricrete along the valley bottoms in the Animas River watershed study area (T.J. Casadevall and D.J. Sofield, written commun., 1996) delineated ferricretes in some parts of the region. Field examination of these outcrops demonstrated the need for refinement of this early mapping and development of a more complete map of ferricrete throughout the watershed (Yager and Bove, this volume, pl. 2).

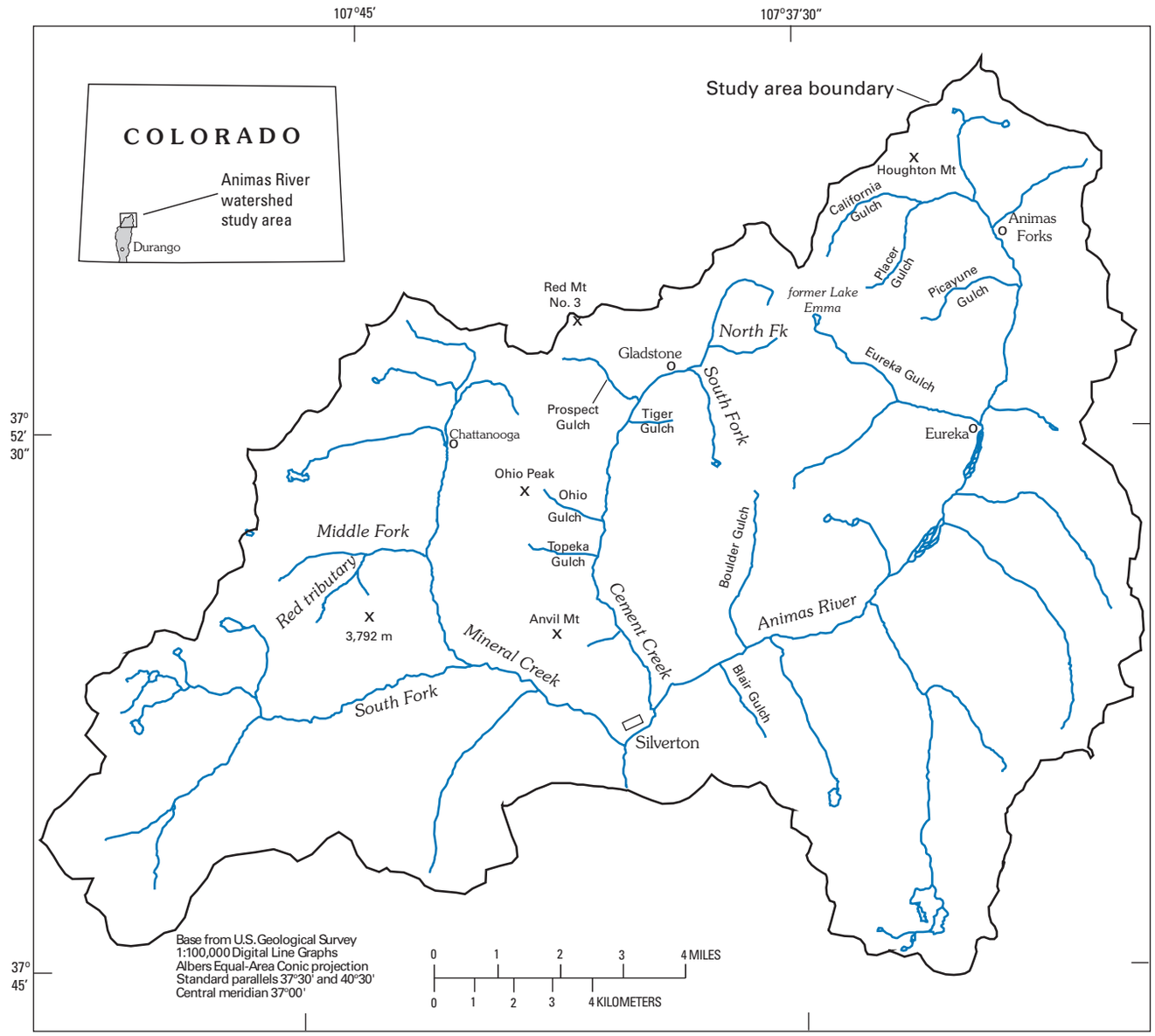

Figure 1. Rivers, creeks, peaks, and towns in the Animas River watershed study area.

Mapping of Ferricretes

In this study, the Mineral and Cement Creek basins were mapped in detail to delineate the extent and lithologic variation of ferricretes. However, because of time limitations, the upper Animas River basin upstream of the town of Silverton was mapped only in reconnaissance. To unravel the complex nature of these sedimentary deposits, we recorded a set of physical properties at each outcrop and compiled them to create a classification scheme (table 1). Important field observations include the presence or absence of clasts, degree of rounding of clasts and their lithologies, grain size, degree of sorting, whether clasts are matrix- or clast-supported, porosity, color, presence of small-scale structures within the deposit, orientation of layering, and dimensions of outcrop. In addition, we noted whether the outcrop was wet or dry, to determine whether the ferricrete deposit might be active. Because of temporal variations in ground-water flow, this observation was not always a definitive determination of recent ground-water activity.

We were able to distinguish and map three primary classes of ferricrete: ferricretes that contained essentially no clasts (that is, spring and bog iron deposits), ferricretes that contained predominantly angular clasts, usually of a single rock type (that is, iron-cemented colluvial deposits), and ferricretes that contained subangular to subrounded or rounded clasts of several lithologies (that is, iron-cemented alluvial deposits). In addition, ferricrete deposits were identified that have a black matrix. These deposits contain elevated amounts of manganese in the iron cement and were mapped as manganese-rich ferricrete deposits or manganocretes.

Table 1. Classification of ferricrete deposits in the Animas River watershed study area.

Class	Description	Location
Alluvial	Iron oxyhydroxide-cemented conglomerate. Clast supported with subangular to subrounded, multi-lithologic clasts coated with iron oxyhydroxides, poor to moderately sorted. Fluvial sedimentary structures and subhorizontal layering observed in some outcrops.	Along stream beds and terraces. Steep valley sides of lower portions of Mineral and Cement Creeks contain exposures as much as 30 m above stream level.
Colluvial	Iron oxyhydroxide cemented, clast supported with angular clasts of limited lithologic variation, poorly to moderately sorted, massive to minor layering subparallel to hillslope.	Steep tributaries, avalanche chutes, and hillslopes.
Iron spring and bog	Few or no clasts, generally contains fine, horizontal lamination with some vertical lamination in feeder zones.	Iron bogs found within valley floors and iron springs feed some bogs, also found along hillslopes near bedrock contacts or fracture zones.
Manganocrete	Term used for ferricretes with black to dark-gray matrix. Includes both clast-supported and matrix-supported deposits.	Manganocrete deposits mapped in upper Animas River basin upstream of Eureka townsite.

Iron Spring and Bog Deposits

Clast-absent, iron-rich ferricretes observed along sections of Mineral and Cement Creeks tend to have two types of morphology. Both these morphological types are designated as bog iron on the ferricrete map (Yager and Bove, this volume, pl. 2). One type consists of dense, laminated iron oxyhydroxide, and forms aprons surrounding active springs (fig. 2). The second type is more porous (as much as 30 percent void space) and crops out along slopes near valley floors (fig. 3).

Active iron spring deposits along valley floors may form iron bogs. In the Mineral Creek basin, large iron bogs are found in beaver ponds at Chattanooga, along the lower portion of a north-flowing tributary of Middle Fork Mineral Creek referred to as Red tributary in Mast, Verplanck, and others (2000); along the east bank of Mineral Creek at the confluence with Middle Fork Mineral Creek; and in beaver ponds along the north bank of South Fork Mineral Creek upstream of the confluence with Mineral Creek (Yager and Bove, this volume, pl. 2). In Cement Creek, iron bog areas include large areas of the flood plain both upstream and downstream of the confluence with South Fork Cement Creek, south of North Fork Cement Creek, upstream of the confluence with Ohio Gulch, and an area on the west side of Cement Creek upstream of Soda Gulch (Yager and Bove, this volume, pl. 2).

Large bog iron deposits (inactive iron bogs) are found along the hillslope southwest of the active Chattanooga bogs on the west side of upper Mineral Creek, in the upper portion of Cement Creek along the east bank upstream of the confluence with North Fork Cement Creek, and in the upper portion of Boulder Gulch (Yager and Bove, this volume, pl. 2). Historically, some of these bog iron deposits were mined and used for flux in smelters (Harrer and Tesch, 1959).

Iron springs that discharge along valley floors form travertine-like terraces that are sporadically coated with algal material. Hydrogeochemical studies of these deposits are described in Stanton, Fey, and others (this volume, Chapter E25). Spring water flows as a thin film over the terraces toward the creek. The terraces consist of iron oxyhydroxides with varying amounts of organic material, including conifer cones and needles, leaf litter, mosses, algae, twigs, and logs. Casts of organic matter preserve fine detail, including bark, wood grain and structure of logs, and algal and moss textures. In cross section, these deposits are horizontally to subhorizontally laminated, some with strong color banding. Sand- to silt-sized rock fragments are incorporated in some laminae and are matrix supported. Some low-lying iron-rich springs have more diffuse outflows, which form iron bogs. These iron bogs often contain a wide variety of algae, and the water has highly variable pH, ranging from 3.5 to near 7. Organic-rich, wet, spongy ground and a distinct flora that includes mosses and sedges characterize these bogs.

The more porous, clast-absent ferricrete deposits have been mapped along the lower sections of the valley sides. Excavation for road building or mineral prospecting has exposed several of these deposits. Spectacular examples crop out on the hillslope west of the Chattanooga bogs (99VM65 on plate 2 of this volume) and in the upper portion of South Fork Cement Creek. (Note that solid sample names from a given site have an “S” (99VMS65) and water sample names from a given site have an “F” (99VMF65).) In contrast to valley-floor deposits, banding in these more porous ferricretes tends to be vertical to subvertical (fig. 3). In the upper section of South Fork Cement Creek, vertically layered deposits crosscut horizontally layered deposits (this volume, fig. 11 of pl. 2). Laminae may be of varying colors, including light and dark brown and yellow. Rock fragments are generally absent. These deposits appear to be paleo-feeder zones to iron-rich springs.

Colluvial Ferricrete

Colluvial ferricretes are clast supported, and the clasts are angular to subangular (fig. 4). These deposits commonly are exposed on hillslopes and may grade into iron bog and spring deposits down gradient where the slope angle decreases. Crude layering defined by alignment of clasts, typical of soil creep, is observed in most outcrops and is subparallel to the

Figure 2. Travertine-like iron spring deposit, east bank of Mineral Creek near confluence with Middle Fork Mineral Creek (site 99VM72).

topography. Iron oxyhydroxides coat the rock fragments and fill void spaces, in places displaying a layered texture. Within a single outcrop, the degree of cementation can vary considerably. Many deposits are poorly sorted, containing pebble- to cobble-sized clasts, which are mainly monolithologic. The range in composition of the clasts is limited to the upslope lithologic variations. Some outcrops are damp, with water coating clasts; ground-water flow is limited to drips from the outcrop. Organic material is limited to soil zones, which generally contain only roots and mosses; however, wood that has been replaced by iron oxide is observed in colluvial ferricretes in Topeka Gulch (SDY 017B), Cement Creek north of Tiger Gulch (99ABFC123), and South Fork Cement Creek (99ABFC163). Good examples of colluvial ferricrete can be seen in the North Fork Cement Creek valley (site IDY0014, this volume, pl. 2).

Alluvial Ferricrete

A third class of ferricrete, alluvial ferricrete, was mapped within and along much of Mineral and Cement Creeks. Lesser amounts of alluvial ferricrete are exposed in the valley of the Animas River upstream of the confluence with Cement Creek. In general, alluvial ferricretes are iron oxide-cemented conglomerates, but in some outcrops, lenses of well-sorted or graded silts and sands are present. The alluvial ferricrete consists of subangular to subrounded or rounded clasts with iron oxides coating the grains and filling void space to varying degrees. Clasts typically are pebble- to cobble-sized with a few boulders. Spaces between clasts are generally filled with finer grained sediment. Some outcrops display clast imbrication that dips upstream. Within an outcrop, variable cementation can create ledges that range from horizontal to subparallel with the valley floor. Cementation appears to be independent of grain size or sedimentary structures.

Some deposits are poorly sorted and may be avalanche or flood deposits. These deposits commonly contain logs that are randomly oriented, along with occasional buried stumps in growth position on the flood plain. At the confluence with tributary streams, alluvial ferricretes generally thicken to incorporate alluvial fan material from the tributaries, such as at the confluence of Prospect Gulch with Cement Creek (Vincent and others, this volume). The percent of void space in alluvial ferricretes is generally low, resulting in rocks that are highly resistant to erosion, but which can be undercut by channel erosion and break off as large coherent blocks from the stream banks.

Outcrops as much as 30 m in height are found along the lower portion of Middle Fork Mineral Creek and along Mineral Creek between the confluences of Middle Fork and South Fork Mineral Creek (fig. 5). Alluvial ferricretes of similar scale are exposed along the valley walls of lower Cement Creek and at the mouth of Blair Gulch on the upper Animas River. Sections of the creek bed in Cement Creek, lower Middle Fork Mineral Creek, Mineral Creek downstream of the confluence with South Fork Mineral Creek, and the Animas River downstream of the confluence with Cement Creek consist of alluvial ferricrete. Much of the town of Silverton is underlain by alluvial ferricrete; it is often the competent rock upon which building foundations rest (Steve Fearn, consulting mining engineer, oral commun., 1998; this volume, fig. 8 of pl. 2). Alluvial ferricrete is actively forming in Red tributary on Middle Fork Mineral Creek (Mast, Verplanck, and others, 2000) at the base of a talus slope (Yager and others,

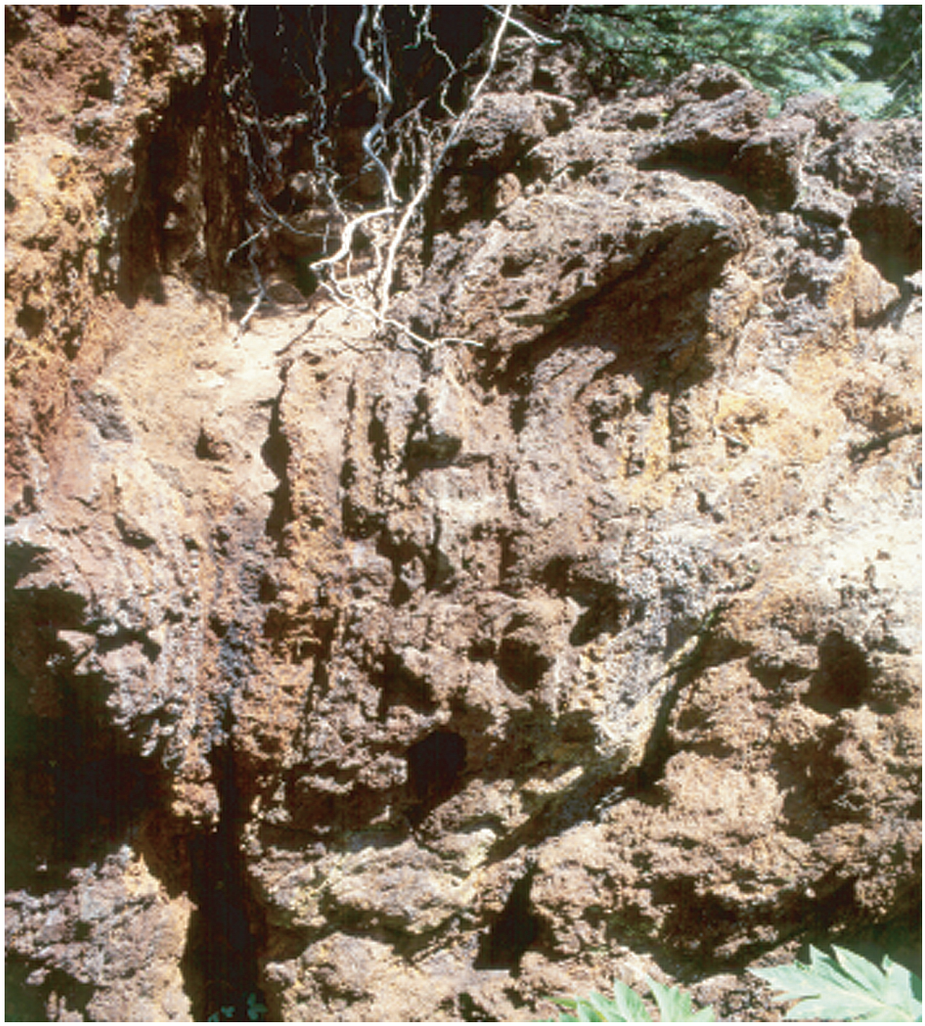

Figure 3. Vertical lamination of porous spring deposit, west side of Mineral Creek upstream of Chattanooga (site 99VM65). Approximately 1 m in height.

2000). This location contains recent avalanche debris that has been cemented by iron oxyhydroxides (fig. 6). Ferricrete is also actively forming in Cement Creek near the confluence of Ohio and Tiger Gulches.

Manganiferous Ferricretes

In the upper Animas River basin upstream of Silverton, outcrops of black oxide-cemented deposits—some clast supported and some matrix supported—are present (fig. 7). Because of the distinct color, these were mapped as manganese-rich ferricrete deposits, herein referred to as manganocretes. Ore deposits in the Eureka graben in this section of the watershed are manganese rich, containing primary pyroxmangite ((Mn, Fe, Ca, Mg)SiO_3) and rhodochrosite ($MnCO_3$) with minor friedelite ($Mn_8Si_6O_{18}$), tephroite (Mn_2SiO_4), and helvite ($Mn_4(Be_3Si_3O_{12})S$) (Casadevall and Ohmoto, 1977). Weathering of the deposits mobilizes manganese; subsequent manganese redeposition results in the formation of manganese oxides. The black color of these deposits is derived from the cement having a significant portion of manganese oxide in it. A suite of these samples was collected and analyzed to determine the relative portions of iron and manganese, as well as trace-element concentrations.

Composition of Deposits

Solid samples of matrix material from the ferricrete and manganocrete deposits were analyzed to determine the mineralogy and chemistry of the various cements. Matrix material was separated from clast-rich samples using a ceramic plate and roller that breaks the cement away from the clast material, thereby minimizing incorporation of rock fragments in the sample to be analyzed. The fine-grained matrix material was concentrated by sieving to <100 mesh. The fine-grained detritus could not be completely removed from the samples,

and some matrix samples still contained detritus that diluted the iron content of the matrix material. Samples were analyzed using mixed-acid total digestion (Briggs, 1996) followed by inductively coupled plasma–atomic emission spectroscopy (ICP-AES). Results are in the database (Sole and others, this volume, Chapter G; D.L. Fey, analyst). Sulfur was analyzed commercially by XRAL Laboratories using high-temperature combustion in a stream of oxygen in the presence of elemental iron. This combustion produces SO_2 gas whose concentration was determined using an infrared detector.

Mineralogy of the matrix samples was determined by X-ray diffraction. Powder patterns were obtained using a Shimadzu diffractometer with Ni-filtered CuK_α radiation scanning from 4° to 60° 2θ. The X-ray spectra were not background-corrected because samples containing weakly crystalline materials such as schwertmannite and poorly ordered goethite cannot be identified if background corrections are made to the spectra. All samples were run blind (Rhonda Driscoll, analyst). Mineralogical results are presented in terms of major, minor, or trace constituents on the basis of the intensity of the major peak in the X-ray spectra. The intensity scale has not been calibrated to determine the percent of the mineral present in the sample. Amorphous iron oxides were presumed to be present in all iron-matrix samples. Where no discrete iron oxide phases were identified in the X-ray diffraction patterns, amorphous iron oxides were indicated as the major iron oxide phase in the database (Sole and others, this volume).

Mineralogical Results

Mineralogical results for the 74 samples analyzed were divided into two categories, iron oxide minerals and rock-forming minerals. Iron oxide minerals included goethite (α-FeO(OH)), schwertmannite ($Fe_8^{III}O_8(SO_4)_{1.25}(OH)_{5.5}$), and amorphous iron oxyhydroxide. Minor or trace amounts of jarosite ($KFe_3^{III}(SO_4)_2(OH)_6$) were found in three samples; trace amounts of pyrite (FeS_2) were observed in one sample. No discrete manganese minerals were detected in the manganocrete samples. Minerals present as fine-grained detrital phases in the matrix included albite, muscovite, orthoclase, and quartz. Identified layer silicates included clinochlore (the magnesium chlorite), montmorillonite, and saponite. Rutile was observed in four samples and boehmite in one sample.

The mineralogy of the active iron spring and bog samples (32 samples) consisted primarily of amorphous iron oxides with identifiable schwertmannite and goethite. Both minerals are common precipitates from acidic drainage; however, schwertmannite is the predominant form when the pH is less than 4.5 and is indicative of more acidic waters (Bigham and others, 1996). Jarosite was observed in a banded ferricrete sample from the soil zone adjacent to the large spring in lower Prospect Gulch. Quartz was common, whereas albite and muscovite were often detected but usually in only minor amounts. Dissolved silica present in the stream waters produced silica gel when filtered (G.A. Desborough, oral commun., 2001).

Figure 4. Poorly to moderately well cemented colluvial ferricrete, north side of Middle Fork Mineral Creek subbasin (site 99VM34).

Figure 5. Alluvial ferricrete, 30 m thick, south bank of Middle Fork Mineral Creek near confluence with mainstem.

Thus, quartz could be detrital or authigenic. Other silicate minerals in these deposits are rare and were found only in trace amounts. The silicate minerals and rutile were likely detrital lithics that were washed or blown into the bogs or springs.

The mineralogy of the inactive iron spring and bog iron deposits (12 samples) did not differ significantly from that just described except that only about half the samples contained identifiable schwertmannite. The mineralogy of the matrix of colluvial ferricrete (10 samples) primarily consisted of goethite and amorphous iron oxides. Quartz was common, and albite and muscovite were present in some samples. Clinochlore and rutile were present in some active colluvial ferricrete samples, and saponite was detected in one sample.

The mineralogy of the alluvial ferricrete deposits (20 samples) differed from that of the active iron spring and bogs in that goethite or amorphous iron oxides were commonly found. Only one sample contained schwertmannite, another jarosite, and a third pyrite. Quartz was ubiquitous. Albite and muscovite were common, and trace amounts of orthoclase and clinochlore each were detected in one sample. Montmorillonite was detected in 6 of the 20 samples analyzed. These minerals probably represented small contributions from lithic fragments that were not completely separated from the matrix. Boehmite, $Al(OH)_3$, was detected in one sample.

Identifiable iron minerals were absent from the manganocrete deposits (eight samples); amorphous iron oxides were presumed to be present. No manganese-bearing minerals, including oxides, were detected in these deposits; thus, amorphous manganese was also presumed to be present. Quartz was ubiquitous. Many samples contained fine-grained clastic material, as shown by the presence of identifiable albite and muscovite in all samples. Clinochlore was identified in four of the eight manganocrete samples, and other rock-forming minerals were identified in minor or trace amounts in the manganocrete samples.

In a laboratory, each sample was dried and compared, under uniform lighting, with Munsell soil color charts (Rhonda Driscoll, analyst). A few general observations can be gleaned from the mineralogical data. In general, the color of the samples varied with mineralogy. Ferricrete matrix samples that contained schwertmannite as a major phase had Munsell soil color indices of 2.5*YR* to 5*YR*. In these samples goethite was also a major phase. The one sample in which schwertmannite was the only major phase had a color index of 2.5*YR* 3/6 (dark red). Most of the ferricrete matrix samples that had goethite as the only major iron phase had color indices of 7.5*YR* to 10*YR*. The range in goethite color is the same range that Bigham and others (1992) noted.

Figure 6. Recent avalanche debris on Red tributary, partially cemented by iron oxyhydroxide precipitates (site SDY9914).

Figure 7. Manganocrete, in spring deposit in California Gulch (site 99VA01).

Schwertmannite was primarily observed in active ferricretes, and goethite was observed in both active ferricretes and paleo-ferricretes. These observations are consistent with previous studies on the formation and preservation of schwertmannite. Experiments by Bigham and others (1996) demonstrated that schwertmannite is a metastable phase and transforms to goethite. For natural schwertmannite in an aqueous solution, the transformation was complete in 1,739 days; and for synthetic schwertmannite, the transformation was complete in 543 days (Bigham and others, 1996).

Chemical Results

Solid-phase chemical analyses of ferricrete and manganocrete matrix samples are tabulated in Wirt and others (this volume) along with chemical results from corresponding water samples. The major-element chemical results from matrix samples are compatible with the mineralogical results in that iron oxide was the most abundant constituent in most samples (FeO ranged from 5.7 to 77.2 weight percent). The black matrix samples had the highest manganese concentrations (MnO greater than about 3 weight percent) and FeO:MnO≈1; only two samples had FeO:MnO<1 (fig. 8).

Two samples (99ABFC170 and 175B) had MnO concentrations greater than 1 percent but were not manganocretes because of their brown color. These samples were from deposits on the east side of Cement Creek upstream of Gladstone (Yager and Bove, this volume, pl. 2). This part of the basin is within the western portion of the Eureka graben, which hosts manganese-rich veins that contain pyroxmangite and rhodochrosite (Casadevall and Ohmoto, 1977). Three other samples (99VMS13A–C) plotted in a field just above the other ferricrete samples because of slightly greater MnO concentrations (fig. 8). These samples were collected along the lower portion of the hillslope west of Mineral Creek at Chattanooga (this volume, pl. 2). Two of these samples were ferricrete matrix exposed above a draining adit, and the third was iron floc from the adit drainage. Although no manganese-rich mineral deposits are known in this part of the watershed, Miocene to Oligocene rhyolitic dikes and quartz latite stocks crop out upgradient, and units with similar ages and compositions are also present in the upper portion of the Animas River valley, upstream of Animas Forks (Luedke and Burbank, 1987). Bove and others (this volume, Chapter E3) have postulated that the Miocene to Oligocene rhyolitic dikes and quartz latite stocks are associated with some of the manganese-rich mineral deposits in the Eureka graben region.

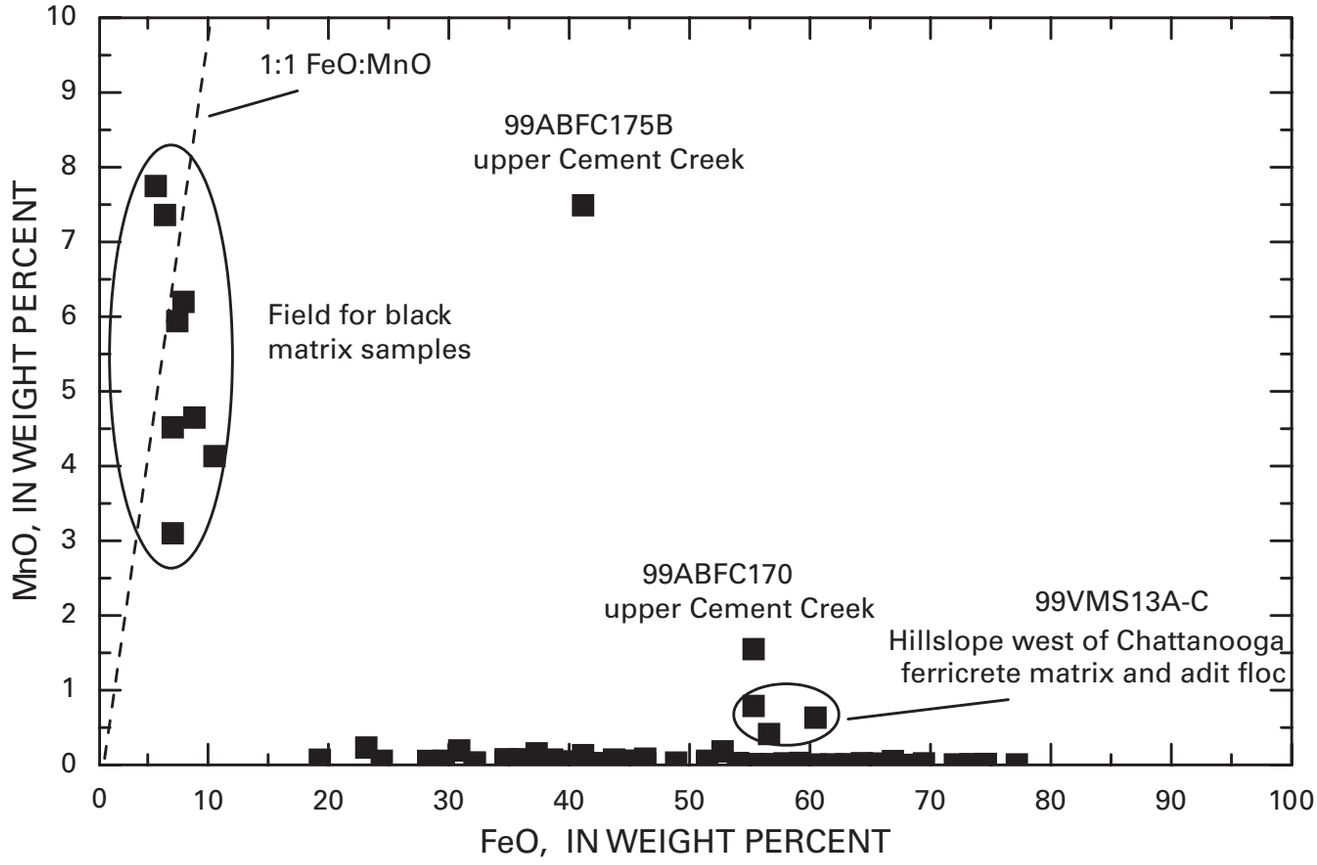

Figure 8. FeO and MnO of ferricrete and manganocrete matrix samples.

Age of the Deposits

More than seventy ^{14}C ages were determined on various materials during the course of our studies in the watershed. The data are compiled and presented in table 2 herein, table 1 in Vincent and others (this volume, Chapter E16), and table 1 in Vincent and Elliott (this volume, Chapter E22). The distribution of ages by basin (fig. 9) and that by material type (fig. 10) are biased, because they reflect the intensity of studies in specific areas. More detailed work was done on both distribution and ages of alluvial ferricrete deposits in the Cement Creek basin than in the other two basins. Wood in alluvial ferricrete deposits was the primary sample type dated. The distribution of peat deposits in the Cement Creek basin was also important in deciphering of the Holocene geomorphological development of Cement Creek (Vincent and others, this volume). The distribution of ages by type of ferricrete deposit is also biased (fig. 10) by limited sampling. As our focus in the Cement Creek basin was on alluvial deposits, we have more age data on alluvial ferricrete than on colluvial ferricrete.

Samples from 34 stumps in growth position or fallen logs were collected for ^{14}C age determinations. We avoided obvious tree roots where their relationship to the surface of the ferricrete or terrace deposit was uncertain. Log samples collected were encased in the ferricrete deposits rather than adhering to or cemented to the side of the outcrop. If an outer decomposed portion was present, we removed it to avoid potential contamination by young carbon. The outer 10–20 rings of large log and stump samples were systematically used for ^{14}C age determinations. Logs and stumps in growth position in alluvial ferricrete were buried during sedimentation, and thus they give the approximate age of deposition of the clastic deposit. Logs that were incorporated in avalanche debris were randomly oriented in the plane of flow within the deposit and most likely were from trees uprooted by the avalanche, thus yielding an age of clastic deposition. Logs in these deposits may be slightly older than the deposit if they died before entrainment in the avalanche debris. In both cases, the ^{14}C ages give the maximum age of cementation and ferricrete formation.

We contracted two commercial laboratories to analyze three different material types: wood or charcoal, cellular matter from peat, and unidentified organic carbon. Methods of sample preparation, analysis, and data reduction are in footnotes in the ^{14}C data tables referred to previously.

Distribution of ^{14}C Ages

Dated wood fragments in alluvial ferricrete have ages that extend from about 5,000 yr B.P. to the present. In contrast, ages of samples from unconsolidated terrace gravel are young, generally less than 500 yr B.P., as expected (fig. 10). The two old stumps in growth position in terrace gravel that were dated were rooted in ferricrete. Presumably, these terrace gravel deposits were not cemented until some time after tree growth began. Dendrochronology of trees on unconsolidated terraces also has shown that uncemented young terraces in the Animas River watershed are common, dating back several hundred years (Church and others, 2000). A significant number of young ^{14}C ages have come from wood fragments cemented in alluvial conglomerates by iron oxides (fig. 10).

Cementation of alluvial deposits may have been a highly variable process. Some outcrops of alluvial ferricrete along both Cement and Mineral Creeks have acid springs containing iron floc. These springs primarily emanate from the base of alluvial deposits along the bedrock contact, but some small seeps emanate from within the deposit, from 1 to 5 m above the creek level. This suggests that some ground water enters the creek near creek level, but that the upper portion of the ferricrete deposit may contain permeable zones where ground-water flow and cementation are occurring. This process can complicate the interpretation of ^{14}C ages on iron-oxide cements. Conversely, the relatively high number of modern ages of logs in ferricrete demonstrates that, in some environments, cementation occurs soon after deposition. In some tributaries, we observed avalanche debris from the previous spring that was coated with iron precipitates the next summer, and which by the second field season was partially cemented.

Twenty-one samples of peat or wood from four different sites within the watershed were dated. In South Fork Mineral Creek peat is actively forming today and has ages ranging from at least 2,000 yr B.P. to the present (table 2). Peat samples dated from the Forest Queen site (Vincent and Elliott, this volume) have ages ranging from at least 3,000 yr B.P. to present. Stanton, Fey, and others (this volume) discuss the wetlands present at the Forest Queen where peat is forming today. A peat deposit at Gladstone has ages as old as 5,000 yr B.P., whereas the peat section studied from near Ohio Gulch has ages as old as 2,500 yr B.P. (Vincent and others, this volume, table 1).

Iron springs and bog iron deposits have a more limited range in age (about 5,000 yr B.P. to present) than the alluvial or colluvial ferricrete deposits (about 9,000 yr B.P. to present; fig. 10). Further, the ages of the iron springs/bog iron, and the colluvial ferricrete deposits are fewer in number than those from alluvial ferricrete. Of the ^{14}C ages in the colluvial ferricrete deposits, only the youngest and the oldest ages are from wood samples. Of the ^{14}C ages from the spring/bog iron deposits, the three youngest ages are from wood samples. All the other ages from colluvial ferricrete and iron spring/bog iron deposits are from unidentified organic carbon extracted from a matrix sample that had a wavy texture, which was identified in the field as a possible algal structure, or from goethite casts containing organic material such as a log.

Table 2. Radiocarbon data for organic carbon in ferricrete samples collected from the Mineral Creek, Cement Creek, and upper Animas River basins, and for wood and peat samples collected from the Mineral Creek basin.

[Note that "B.C." and "A.D." are both placed before dates in this table—for better readability and quicker recognition]

Field No.	Lab No.[1]	$\delta^{13}C_{PDB}$ ‰[2]	^{14}C age years B.P.[3]	Calibrated ages[4]			Comments	Locality (lat N., long W.)
				Intercept(s)[5]	1-sigma range[6]	2-sigma range[6]		
Mineral Creek								
Organic carbon from ferricrete deposits on west side Mineral Creek:								
SDY9827C	GX-26687-AMS	–23.3	4,200±40	B.C. 2876	B.C. 2882–2701	B.C. 2895–2624	Samples from large alluvial ferricrete deposit on west side of Mineral Creek between Middle and South Forks. Stratigraphic order is A–C (top to bottom).	37.8375° N. 107.7276° W.
SDY9827A	GX-26685-AMS	–21.1	4,460±40	B.C. 3097	B.C. 3328–3028	B.C. 3346–2924		37.8375° N. 107.7275° W.
SDY9827B	GX-26686-AMS	–22.9	5,600±40	B.C. 4452–4404	B.C. 4460–4360	B.C. 4518–4347		37.8375° N. 107.7275° W.
99VMS65	GX-26691	–24.4	4,820±360	B.C. 3640	B.C. 3980–3100	B.C. 4360–2600	Iron spring deposit, upstream from Middle Fork Mineral Creek.	37.8653° N. 107.7267° W.
Middle Fork Mineral Creek								
Samples of wood in terrace deposits:								
00ABFC201	B-147007	–25*	790±70	A.D. 1260	A.D. 1190–1280	A.D. 1050–1100 A.D. 1140–1300	8 in. diameter log in alluvial ferricrete about 2.5 ft above low-flow water level.	37.8448° N. 107.7318° W.
00ABFC202A	B-147008	–25*	870±50	A.D. 1180	A.D. 1060–1230	A.D. 1030–1270	8 in. diameter log in colluvial ferricrete at low-flow water level.	37.8441° N. 107.7290° W.
00ABFC200	B-147006	–25*	4,520±70	B.C. 3340–3200	B.C. 3360–3090	B.C. 3500–3460 B.C. 3380–3000 B.C. 2980–2940	Wood in alluvial ferricrete 4 ft above low-flow water level.	37.8451° N. 107.7323° W.
Organic carbon from ferricrete deposits:								
99VMS33	GX-26690-AMS	–23.8	2,760±40	B.C. 902	B.C. 969–834	B.C. 1001–825	Ferricrete matrix sample from 40 ft up in glacial outwash deposit, lower Mineral Creek.	37.8449° N. 107.7310° W.
ODY9815A	GX-26688-AMS	–24.9	2,790±30	B.C. 966–921	B.C. 995–901	B.C. 1004–835	Colluvial ferricrete matrix sample from Red tributary.	37.8350° N. 107.7532° W.
SVFFC	GX-27519-AMS	–23.2	4,390±30	B.C. 3017–2940	B.C. 3082–2921	B.C. 3097–2914	Filamentous ferricrete matrix sample downstream from Bonner mine.	37.8448° N. 107.7310° W.
South Fork Mineral Creek								
Samples of peat:								
97ABS321B	GX-27696	–26.5	710±40	A.D. 1287	A.D. 1287–1298	A.D. 1258–1386	Peat from 12 in. depth in core through active peat bog.	37.8143° N. 107.7367° W.
97ABS322A	GX-27697	–28.0	1,060±130	A.D. 990	A.D. 780–1160	A.D. 680–1260	Peat from 21 to 31 in. depth in core through active peat bog.	37.8141° N. 107.7364° W.

Table 2. Radiocarbon data for organic carbon in ferricrete samples collected from the Mineral Creek, Cement Creek, and upper Animas River basins, and for wood and peat samples collected from the Mineral Creek basin.—Continued

Field No.	Lab No.[1]	$\delta^{13}C_{PDB}$ ‰[2]	^{14}C age years B.P.[3]	Calibrated ages[4]			Comments	Locality (lat N., long W.)
				Intercept(s)[5]	1-sigma range[6]	2-sigma range[6]		
South Fork Mineral Creek—Continued								
Samples of peat from iron-rich bog sediments:								
97-ABS319	GX-27698	–24.1	1,480±40	A.D. 600	A.D. 541–639	A.D. 444–655	Peat from 8 in. depth in core through active iron bog forming in peat deposit.	37.8163° N. 107.7298° W.
97ABS320C	GX-27699	–25.4	1,920±190	A.D. 80	160 B.C.–A.D. 340	40 B.C.–A.D. 540	Peat from 12 in. depth in core through active iron bog forming in peat deposit.	37.8316° N. 107.7298° W.
Organic carbon from ferricrete deposits:								
SDY9813A	GX-26682-AMS	–25.2	1,170±40	A.D. 887	A.D. 780–943	A.D. 729–980	Colluvial ferricrete matrix from bottom of stratigraphic sequence.	37.8215° N. 107.7443° W.
SDY9813B	GX-26683	–24.4	4,430±390	B.C. 3090–3030	B.C. 3640–2500	B.C. 3990–1980	Colluvial ferricrete matrix from top of stratigraphic sequence.	37.8215° N. 107.7443° W.
Cement Creek basin								
Organic carbon from casts in ferricrete deposits:								
99ABFC139B	GX-26391	–23.3	5,000±190	B.C. 3780	B.C. 3980–3640	B.C. 4250–3370	Iron spring deposit, cast was not identifiable.	37.8546° N. 107.6762° W.
99ABFC163C Total	GX-27515	–22.4	6,010±70	B.C. 4900–4850	B.C. 4990–4800	B.C. 5190–4720	Log in colluvial ferricrete deposit that has been totally replaced by goethite (bulk sample).	37.8763° N. 107.6441° W.
99ABFC163C Fulvic	GX-27971-AMS	–25.4	2,720±30	B.C. 887–834	B.C. 900–828	B.C. 965–807	Fulvic acid component extracted from sample.	
99ABFC163C Humic	GX-27972-AMS	–27.0	2,080±40	B.C. 91–61	168 B.C.–A.D. 6	199 B.C.–A.D. 17	Humic acid component extracted from sample.	
99ABFC163C Residual	GX-28131	–23.6	5,410±220	B.C. 4320–4252	B.C. 4458–3979	B.C. 4766–4759 B.C. 4716–3756 B.C. 3744–3726 B.C. 3725–3712	Residual cellular carbon remaining after extraction of organic acids.	
99ABFC123C	GX-26390	–23.3	7,680±200	B.C. 6470	B.C. 6690–6270	B.C. 7060–6090	Goethite replaced log in colluvial ferricrete.	37.8787° N. 107.6685° W.
Organic carbon from ferricrete deposits, Topeka Gulch:								
SDY0017A	GX-27517-AMS	–22.7	24,020±100	Outside of calibration range			Finely laminated matrix in bog iron deposit.	37.8496° N. 107.6897° W.
SDY0017B	GX-27518-AMS	–26.3	3,950±40	B.C. 2466	B.C. 2545–2410	B.C. 2569–2309	Ferricrete matrix from colluvial deposit.	37.8494° N. 107.6897° W.

Table 2. Radiocarbon data for organic carbon in ferricrete samples collected from the Mineral Creek, Cement Creek, and upper Animas River basins, and for wood and peat samples collected from the Mineral Creek basin.—Continued

Field No.	Lab No.[1]	$\delta^{13}C_{PDB}$ ‰[2]	^{14}C age years B.P.[3]	Calibrated ages[4]			Comments	Locality (lat N., long W.)
				Intercept(s)[5]	1-sigma range[6]	2-sigma range[6]		
Upper Animas River basin								
Organic carbon from manganocrete samples, California Gulch:								
SVMCS	GX-27520-AMS	–25.1	1,590±40	A.D. 433	A.D. 420–537	A.D. 393–595	Matrix from manganiferous colluvial ferricrete from talus fan.	37.9242° N. 107.6089° W.
Organic carbon from manganocrete samples, Eureka Gulch:								
HPDY0016	GX-27516-AMS	–22.8	8,000±40	B.C. 7055–6870	B.C. 7055–6828	B.C. 7062–6703	Matrix from manganiferous colluvial ferricrete from talus fan.	37.9046° N. 107.6751° W.
Animas River basin, downstream from Silverton								
Charcoal from Elk Park:								
01ABS126C1	GX-28384	–23.3	2,930±130	B.C. 1190–1130	B.C. 1370–1340 B.C. 1320–970	B.C. 1490–1480 B.C. 1440–820	Charcoal from depth of 18 in. below base of tailings deposited during Gladstone flood (Oct. 5, 1911).	37.7275° N. 107.6559° W.

[1]Radiocarbon data have been obtained from two commercial laboratories, Beta Analytic Inc. (Lab. No. B-xxxxxx) and Geochron Laboratories (Lab. No. GX-xxxxx). Some of the analyses were done using accelerator mass spectrometry (AMS) where the amount of carbon was small. Some of the $^{13}C/^{12}C$ data for samples marked with an asterisk (*) were not measured and were estimated to be –25 ‰ (per mil) based on values typical of this type of material.

[2]Carbon isotopic composition relative to Peedee belemnite (PDB) in per mil (‰).

[3]Conventional radiocarbon age (^{13}C corrected) based on the Libby half life (5,570 years) for ^{14}C, as reported by the laboratory in years before A.D. 1950 (B.P.). The error is ± 1 sigma as judged by the analytical data alone. The sample was crushed if necessary and dispersed in water. The eluted clay/organic fraction was treated in hot dilute 1N HCl to remove any carbonates. It was then filtered, washed, dried, and combusted in oxygen to recover carbon dioxide for analysis.

[4]Ages calibrated using the CALIB4.3 program based on Stuiver and Reimer (1993) with data from Stuiver and Braziunas (1993) and Stuiver and others (1998). The 1998 atmospheric decadal data set and laboratory error multiplier K=1 were used in the calculations.

[5]Maximum and minimum values given if the radiocarbon age intercepted the calibration curve at multiple locations. Dates rounded to the nearest decade if the standard deviation in the radiocarbon date was ≥50 years.

[6]Calibrated age range (or the maximum and minimum if there was more than one range) using the intercept method. Dates rounded to the nearest decade if the standard deviation in the radiocarbon date was ≥50 years. 1 sigma = square root of (sample standard deviation^2 + curve standard deviation^2); 2 sigma = 2 × square root of (sample standard deviation^2+ curve standard deviation^2).

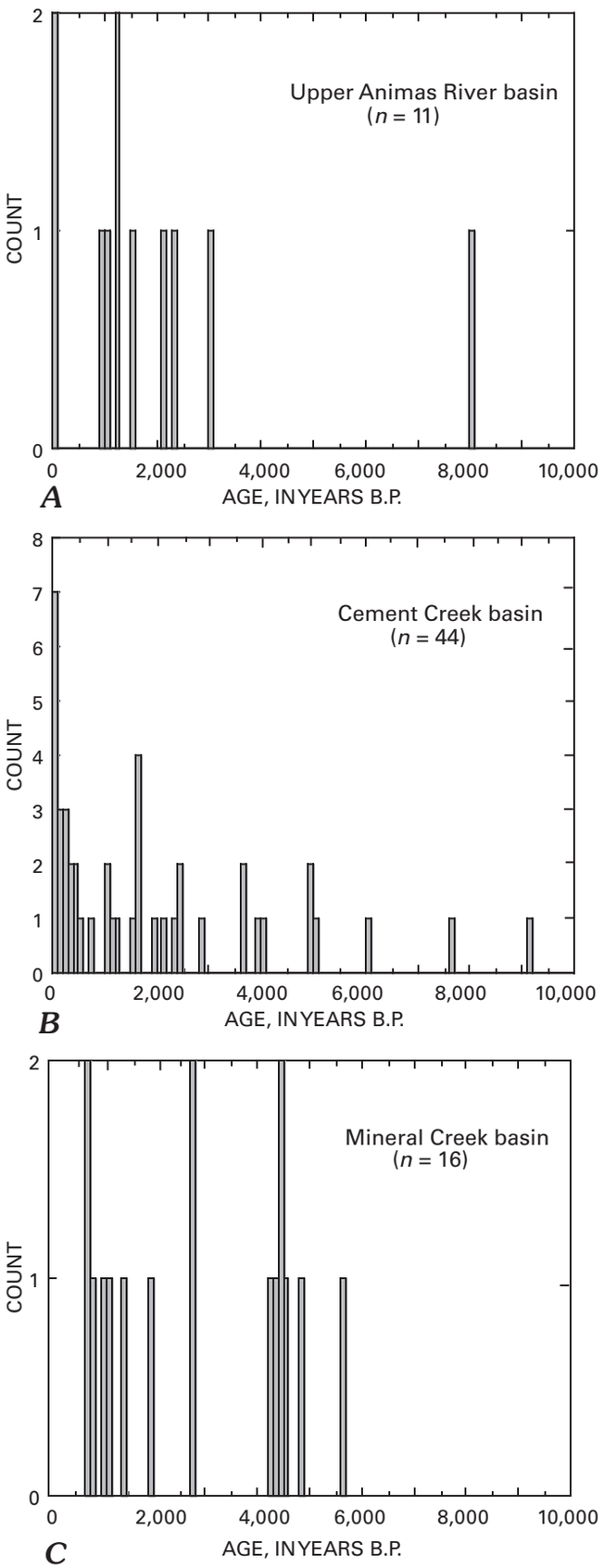

^{14}C Ages Determined in "Unidentified Organic Carbon"

Logs could not be found in alluvial ferricrete at some important localities—specifically, the 20–30 m thick ferricrete deposits along the valley walls of the lower portion of Middle Fork Mineral Creek, Mineral Creek downstream from the confluence with Middle Fork Mineral Creek, lower Cement Creek downstream from the confluence with Soda Gulch, and at the confluence of Blair Gulch with the Animas River (Yager and Bove, this volume, pl. 2). To determine the age of ferricrete formation in these thick deposits, unidentified organic carbon from iron-oxide casts of algal material was sampled from a block of ferricrete approximately 13 m above stream level in the Mineral Creek section (sample 99VMS33). The shape of the casts resembled the morphology of the filamentous algae *Ulothrix* observed in acidic seeps near the base of the outcrop. The ^{14}C age of this sample was 2,760±40 yr B.P. (GX-26690-AMS, table 2) and could define the time of cementation. Other ages from unidentified organic carbon samples (table 2) appear enigmatic, and thus we tried to test the reliability of using dates from unidentified organic carbon samples.

In order to evaluate the reliability of ages obtained from "unidentified organic carbon," we extracted different organic phases from a goethite-replaced log from site 99ABFC163C on South Fork Cement Creek (this volume, pl. 2). We determined four ^{14}C ages on different organic carbon fractions and the residue. From these data we determined that the ^{14}C system was behaving as an open system in cases where we dated "unidentified organic carbon." The results of this experiment are in table 2; sample preparation and extraction procedures follow.

For the "bulk" ^{14}C age, the iron-oxide matrix was leached with hot (100°–150°C) 1N HCl to remove any mineral (carbonate) carbon. Generally, mineral carbon in the iron-oxide samples did not exceed about 0.25 weight percent. The organic carbon remaining after the leach was then combusted for ^{14}C analysis. The results include components of fulvic and humic acids trapped in the goethite as well as the cellular carbon preserved in the replaced log. The ^{14}C age for the bulk sample 163C (replaced woody material) was 6,010±70 yr B.P. (GX-27515, table 2). A second aliquot of sample (99ABFC163C) was subjected to a humic-fulvic extraction, and these organic fractions were also dated. Humic and fulvic fractions represent the products of degradative and synthetic reactions involving organic substances and are major components of the pool of organic matter. The humic and fulvic fractions were first extracted using 0.1 N NaOH for 24 hours at room temperature with shaking. The solution was separated from the solids by centrifugation and

Figure 9. Distribution of new ^{14}C ages by basin. *A*, upper Animas River basin; *B*, Cement Creek basin; *C*, Mineral Creek basin.

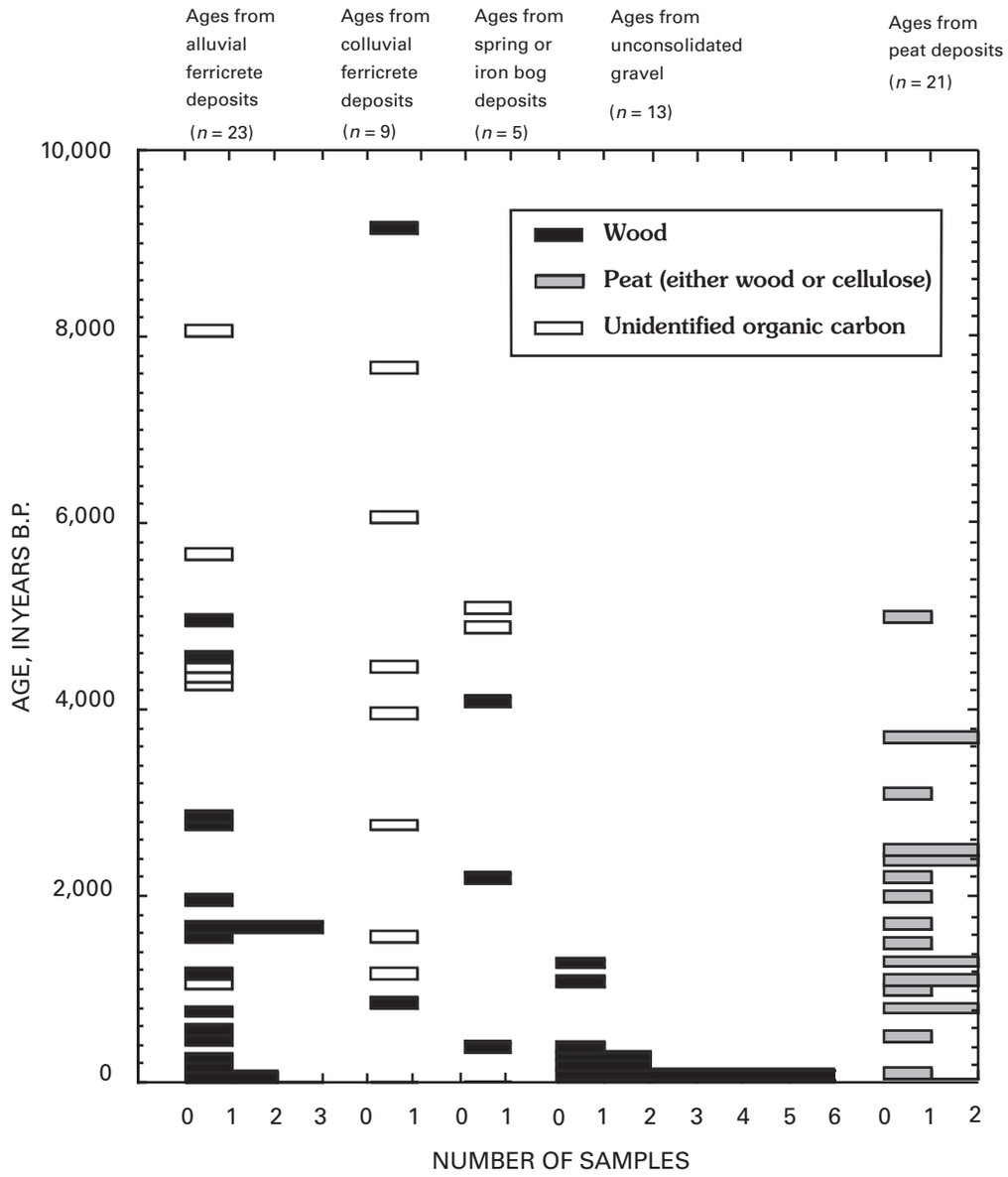

Figure 10. Distribution of ^{14}C by deposit type. Samples displayed by type of material dated and include wood, peat (twigs or cellulose), and unidentified organic carbon. Ages of organic material in clastic deposits date the time of deposition and thus are maximum ages of iron cementation.

then acidified to pH 2 with 1N HCl to precipitate the humic fraction. After filtration and removal of the solid humic precipitate, fulvic fraction was precipitated by adjusting the pH upwards to >5 with 1 N NaOH. The ^{14}C age from the humic fraction precipitate was 2,080±40 yr B.P. (GX-27972-AMS, table 2), and the ^{14}C age from the fulvic fraction precipitate was 2,720±30 yr B.P. (GX27971-AMS). Analysis of the residual carbon remaining in the goethite sample following extraction of the humic and fulvic fractions gave an age of 5,410±220 yr B.P. (GX-28131, table 2). If the carbon in the goethite-replaced log had behaved as a closed system, the residual age would have had to be older than the "bulk" age of 6,010±70 yr B.P. The fact that both the humic and fulvic fractions gave ages that were both different and younger than the ^{14}C age from the "bulk" sample indicated open-system behavior and thus, the ^{14}C age from the "bulk" sample age represents a minimum age for the wood carbon preserved in the goethite matrix of the replaced log.

The extraction method and the fact that ^{14}C ages from the humic and fulvic fractions were similar suggest that a pool of mobile carbon is present in the iron-oxide matrix. Terrestrial humic and fulvic substances originate from the decay of plant materials. The $\delta^{13}C$ composition of terrestrial plant material ranges from –24 to –34 per mil ($^{o}/_{oo}$; Faure, 1986).

Values within this range were obtained for humic (–27.0 $^{o}/_{oo}$) and fulvic (–25.4 $^{o}/_{oo}$) fractions. The "bulk" sample was slightly outside of this range at –22.4 $^{o}/_{oo}$, indicating perhaps some dilution by lichen or algal materials (which have lower ranges of $\delta^{13}C$, –12 to –23 $^{o}/_{oo}$; Faure, 1986). Furniss and others (1999) reported ages of organic carbon from pine needles and leaf litter preserved in iron bog deposits in the New World mining district in south-central Montana and obtained ^{14}C ages in reasonable agreement with the onset of deglaciation (late Pinedale) in northern Yellowstone National Park. However, ages of unidentified organic carbon in colluvial ferricretes could in part result from unidentified organic carbon transported through the system by ground water. Whereas we do not reject the "unidentified organic carbon" ages outright, we have little confidence in them except as minimum ages for the original carbon in the replaced sample.

Basin-Wide Implications

Results from ^{14}C age determinations in this study are complementary to those from previous investigations. Andrews and others (1975) presented age determinations from wood fragments in peat bogs located in Eureka and Picayune Gulches (upper Animas River basin), Elias and others (1991) summarized previous ^{14}C data obtained from former Lake Emma sediments, and Carrara and others (1991) published ^{14}C data from bogs in California Gulch and Eureka Gulch in the upper Animas River basin. Figure 11, a histogram of the ages from ninety-nine ^{14}C ages from wood, summarizes results from our study and previous investigations. Excluded from this compilation are the ^{14}C ages of about 15,000 yr B.P. from moss fragments recovered from former Lake Emma sediments. Elias and others (1991) rejected these

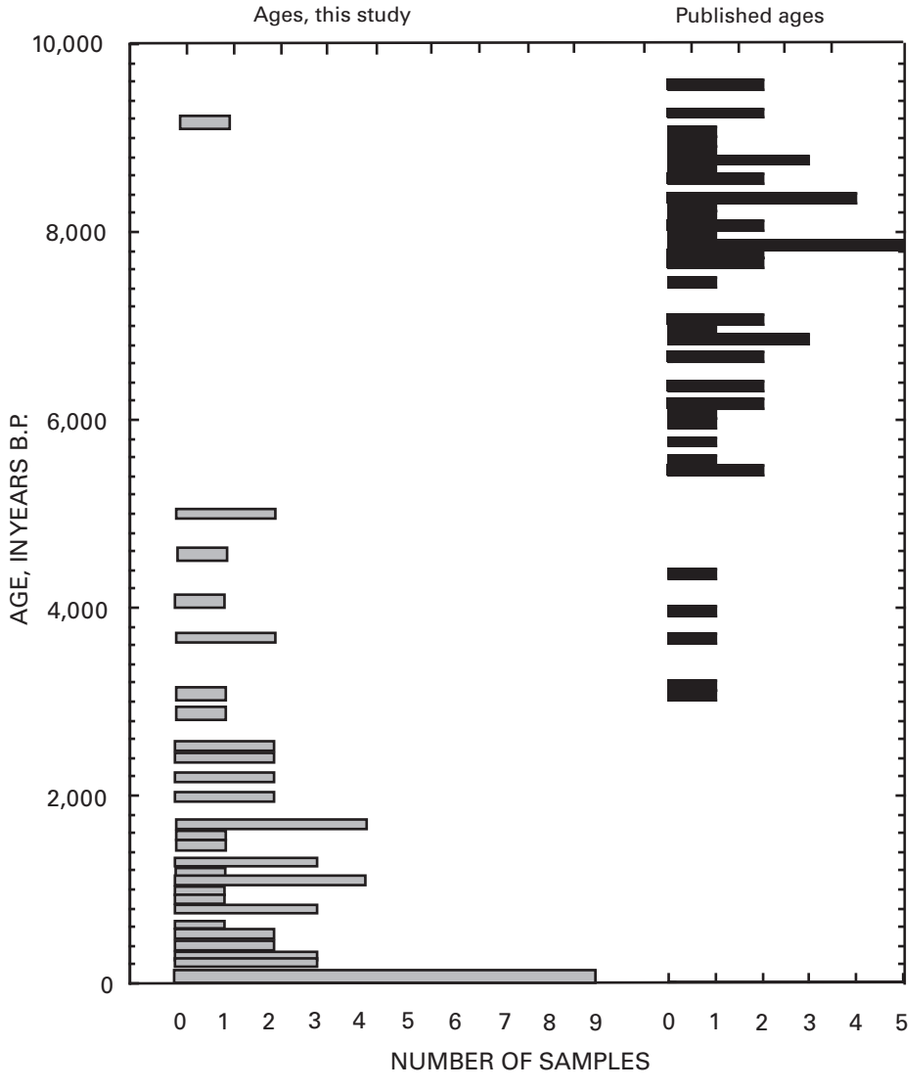

Figure 11. Distribution of all ^{14}C ages. Dates from wood and peat in Animas River watershed study area; age distribution spans entire age range of the Holocene. Published data from Elias and others (1991 and references therein).

older ages from moss because they were inconsistent with ^{14}C ages from insect remains and wood from the same stratigraphic horizons.

Carrara and others (1991) used ages from conifer wood fragments to constrain treeline changes in the Holocene, and Fall (1997) interpreted timberline variations in the region using pollen and plant macrofossil samples from a suite of bog samples in the southern Rocky Mountains of Colorado. At present, timberline (the upper altitude of upright trees) in the southern Rocky Mountains is between 3,535 and 3,600 m, and treeline (small, scattered, windswept trees) is at about 3,660 m (Carrara and others, 1991; Fall, 1997). Fall (1997) demonstrated that timberline was approximately 300 to 700 m below the present timberline at 11,000 yr B.P. and was approximately 270 m higher than present between 9,000 and 4,000 yr B.P. Carrara and others (1991) documented that in the San Juan Mountains, treeline was at least 75 m higher than present from 9,600 to 5,400 yr B.P. The thick alluvial ferricrete deposits that do not contain logs could have been deposited when timberline was lower (about 11,000 yr B.P). The volume of these deposits is consistent with a late glacial outwash setting, and the upper portions of these deposits crop out at an elevation of 3,075 m, which is above the early Holocene timberline (Carrara and others, 1991; Fall, 1997). Carrara and others (1991) postulated that timberline has moved down over the last 5,000 years to its present position. More recent work by Fall (1997) suggests that after 4,000 yr B.P., timberline began to retreat, and the modern climatic regime was established approximately 2,000 yr B.P. That peat bogs started forming before 2,000–5,000 yr B.P. and continue to form shows that the climate within the Animas River watershed study area has been relatively stable since the late Holocene.

The summary of ^{14}C ages from wood fragments in figure 11 shows that the physiography of the Animas River watershed study area has been relatively stable through the Holocene. Studies of the distribution of ferricrete (this volume, pl. 2) and the stability of the Cement Creek stream channel over the last several thousand years (Vincent and others, this volume) are interpreted to indicate that the fundamental weathering and erosion processes active in the formation of the landscape today are representative of those active throughout the Holocene. Ferricrete deposits are the product of those weathering processes and span the last 10,000 years of surficial history in the study area.

Distribution of Ferricrete Deposits

Ferricrete deposits are not evenly distributed within the Animas River watershed study area but crop out in conjunction with specific geologic and geomorphologic features. In general, ferricrete and manganocrete form in surficial deposits on or down gradient from mineralized bedrock, fractures, or veins. In addition, most ferricrete deposits are found within or down gradient from parts of the watershed where hydrothermal alteration was most intense.

Alluvial ferricretes were mapped along most of the valley floor in Mineral Creek downstream of Middle Fork to the confluence with the Animas River. Similarly, in Cement Creek alluvial ferricretes were mapped in the valley floor from Gladstone to the town of Silverton. Only one outcrop of alluvial ferricrete was mapped in the Animas River valley upstream of the confluence with Cement Creek. However, manganocretes were mapped along the valley floors in Placer, California, and Eureka Gulches. Iron spring and bog deposits were mapped along many of the reaches in Cement and Mineral Creeks that contained alluvial ferricretes. Some of these deposits were located in the valley floor and others along lower parts of the valley walls. Colluvial ferricretes were mapped along tributaries to Mineral and Cement Creeks that drain peak 3,792 m, Anvil Mountain, Ohio Peak, and Red Mountain No. 3.

Ferricretes in the Mineral Creek basin provide good examples of how the distribution of ferricrete deposits is closely related to bedrock geology and alteration intensity. No ferricrete deposits were mapped in the Red Mountain district upstream of Chattanooga, although some of the richest silver ore in the watershed study area was mined in the Red Mountain district. The mineral deposits of the Red Mountain district consist of base-metal ores within breccia pipes that intruded along fractures in the Silverton Volcanics (Burbank and others, 1972). Much of the district is characterized by intense acid-sulfate alteration, but the western part of the district that drains into the Mineral Creek basin is propylitically altered with more intense alteration adjacent only to individual breccia pipes (Fisher and Leedy, 1973). The propylitically altered volcanic rocks contain pyrite but do not tend to produce iron-rich drainage (Mast and others, this volume, Chapter E7). Upstream of Chattanooga most of the springs are circumneutral (pH 6.54–7.69) and contain low iron concentrations, generally <0.040 mg/L (Mast, Evans, and others, 2000).

At Chattanooga, an iron-rich sedge bog lies in the valley floor, and paleo-iron spring deposits crop out along the west side of the valley. This locality marks the intersection of the structural margin of the Silverton caldera and a series of east-west-trending faults (Luedke, 1975); it is also within a more intensely altered part of the basin (Bove and others, this volume). Downstream of Chattanooga, no ferricrete deposits were observed until near the confluence with Middle Fork Mineral Creek.

The reach of Mineral Creek between its confluences with Middle and South Forks contains alluvial ferricretes and numerous acidic springs and seeps on both sides of the creek. The east side of this reach is dominated by Anvil Mountain, an acid-sulfate altered zone (Bove and others, this volume). The west side consists of peak 3,792 m, a low-grade copper-molybdenum porphyry deposit, characterized by a zoned alteration pattern with propylitically altered rocks near the periphery and quartz-sericite-pyrite alteration at the center (Ringrose, 1982). In addition, this reach follows the structural margin of the Silverton caldera. Most of the non-mining-affected spring and stream water draining Anvil Mountain and peak 3,792 m

is acidic (pH 2.99–4.92); dissolved iron concentrations range from 0.4 to 120 mg/L (Mast, Evans, and others, 2000). Colluvial ferricretes were mapped along hillslopes or small tributaries in this reach (Yager and Bove, this volume, pl. 2). Note that some outcrops of colluvial ferricrete are too small to map at the 1:24,000 scale.

Similar to Mineral Creek, alluvial ferricretes along Cement Creek tend to form adjacent to or down gradient to bedrock where hydrothermally alteration was most intense. Colluvial ferricretes were primarily mapped within acid-sulfate altered areas, including Anvil Mountain, Ohio Peak, and Red Mountain No. 3. In the upper Animas River basin upstream of the confluence of Cement Creek, few ferricretes were observed. The reach of the Animas River between the confluence of Cement Creek and Eureka townsite follows the structural margin of the Silverton caldera and is dominantly surrounded by propylitized volcanics. The scarcity of ferricrete deposits in this area may be interpreted to indicate that basin-scale structures are not solely responsible for the formation of ferricrete deposits.

Upstream from Eureka, numerous manganocrete deposits were mapped. Manganocrete crops out commonly as finer grained colluvial and alluvial deposits in drainage areas located downstream from weathered, manganese-rich, pyroxmangite- and rhodochrosite-bearing vein structures associated with the Eureka graben. These manganocrete deposits overlie the northwest-trending Sunnyside fault where sulfide-rich polymetallic, base-metal veins formed along the north edge of the Eureka graben (Burbank and Luedke, 1969; Yager and Bove, this volume, pl. 1). California Gulch, Eureka Gulch, and Placer Gulch drain the central region of the Eureka graben near the northeast-trending Sunnyside fault. Alluvial fans and colluvium in the California, Eureka, and Placer Gulch valley floors provide porous and permeable pathways for transport and precipitation of the manganese-rich fluids draining from the veins.

The distribution of ferricrete and manganocrete in the study area highlights the link between pyritic host rocks, acid water, and ferricrete localities and manganese-rich mineral deposits and manganocrete localities. Detailed descriptions of the possible processes that lead to the formation of ferricrete and manganocrete are presented in Wirt and others (this volume); an overview of the scenarios that lead to ferricrete formation instead of manganocrete follows. To form ferricretes, a source of iron is needed. Elevated ferrous-iron concentrations are found in ground water associated with parts of the study area where hydrothermal alteration was intense; geochemical modeling supports the conclusion that the dissolved iron is derived from oxidation of pyrite (Mast, Verplanck, and others, 2000; Bove and others, 2000). In acid water, iron in the ferrous state is highly soluble, but with the addition of oxygen, ferrous iron oxidizes and transforms to ferric iron. Ferric iron is less soluble, which leads to precipitation of iron oxyhydroxides. Two processes that provide oxygen to ground water are (1) ground water emanates from springs and contacts atmospheric oxygen and (2) ground water mixes with oxygenated surface water. Dissolved oxygen in most surface water in the study area is at saturation (Mast, Evans, and others, 2000). Ferricrete forms where these iron precipitates accumulate on surfaces, which can include colluvial and alluvial deposits as well as land surfaces adjacent to springs. Evaporation and hardening of iron-rich crusts are likely an important part of a preservation process.

To form manganocrete, a source of manganese is essential. Polymetallic vein deposits were mined in much of the study area, but some veins, primarily in the upper Animas River basin upstream of the confluence with Cement Creek, contain abundant manganese minerals (Casadevall and Ohmoto, 1977; Nash, 1999). This type of polymetallic vein deposit has a much smaller alteration halo than do the porphyry and breccia types in Mineral Creek basin (Nash, 1999), and spring samples in this part of the study area tended to have higher pH values, higher manganese concentrations, and lower iron concentrations than did springs in the parts of the study area with more intense hydrothermal alteration (Mast, Evans, and others, 2000). In aqueous solutions manganese exists as the Mn^{2+} ion, but with the addition of oxygen, manganese can form insoluble oxides (MnO_2, Mn_2O_3, and Mn_3O_4) depending on pH and Eh conditions. Overall, the processes that lead to the formation of either ferricrete or manganocrete are similar; they entail the weathering of iron or manganese minerals, the transport of dissolved iron or manganese in a reduced state, and precipitation of iron or manganese in an oxidizing environment. Source water composition and redox variations appear to be the primary reasons why manganocrete or ferricrete is formed.

Conclusions

A classification scheme of ferricrete deposits based on physical properties has been developed in the Animas River watershed study area, and three types of deposits have been mapped and characterized. Spring and bog iron deposits contain essentially no clasts and mainly form along valley floors or near the base of the valley walls. Colluvial ferricretes contain predominantly angular clasts, usually of a single rock type, and most form on hillslopes. Alluvial ferricrete deposits are characterized by subangular to rounded clasts of several lithologies and may contain sedimentary structures. These deposits crop out along valley floors or form steep walls in some downcut stream reaches. Deposits that have a black matrix were mapped as manganocrete.

The chemical composition of the ferricrete matrix is dominantly iron, ranging from 5.7 to 77.2 wt. percent FeO, and comprises variable proportions of amorphous iron oxides, schwertmannite, and goethite. In addition, jarosite was identified in a few samples. Ferricrete deposits tend to form within or down gradient from rocks where hydrothermal alteration is most intense.

The matrix of the manganocrete samples contains 3.1–7.7 wt. percent MnO and is amorphous. Manganocrete deposits primarily crop out along the upper Animas River and its tributaries upstream of the town of Eureka, where polymetallic veins containing primary manganese minerals are weathered and oxidized, releasing manganese to ground and surface water. A few other ferricrete matrix samples containing elevated manganese concentrations were located near manganese-rich veins or outcrops of a lithology associated with manganese-rich veins.

Carbon-14 ages from wood fragments within ferricrete deposits ranged in age from 9,150±50 yr B.P. to modern. Ages of logs encased in alluvial and colluvial ferricretes represent the age of clastic deposition and are thus a maximum age of cementation. Some of the outcrops are dry and above creek level, indicating that cementation did not occur recently. Carbon-14 ages from peat and wood from active bogs ranged from 5,000 yr B.P. to modern. Although our new age determinations span the Holocene, most of the ages are less than 5,000 yr B.P., likely reflecting the difficulty in preservation of older deposits in the valley floor and the likelihood that the oldest deposits, outwash and old fans, did not contain wood because treeline was lower during this time. In the study area, ferricrete deposits are a product of weathering processes that span the last 10,000 years and are evidence that, in parts of the study area, iron-rich water flowed prior to the onset of historical mining late in the 19th century.

References Cited

Andrews, J.T., Carrara, P.E., King, F.B., and Stuckenrath, Robert, 1975, Holocene environmental changes in the Alpine Zone, northern San Juan Mountains, Colorado; evidence from bog stratigraphy and palynology: Quaternary Research, v. 5, p. 173–197.

Battiau-Queney, Yvonne, 1996, A tentative classification of paleoweathering formations based on geomorphological criteria, *in* Bouchard, Mireille, and Schmitt, J.-M., eds., Paleoweathering and paleolandforms: Amsterdam, Elsevier, p. 87–102.

Bigham, J.M., Schwertmann, Udo, and Carlson, Liisa, 1992, Mineralogy of precipitates formed by biogeochemical oxidation of Fe(II) in mine drainage, *in* Skinner, H.C.W., and Fitzpatrick, R.W., eds., Biomineralization processes of iron and manganese—Modern and ancient environments: Catena Supplement, Cremlingen-Destedt, v. 21, p. 219–232.

Bigham, J.M., Schwertmann, Udo, Traina, S.J., Winland, R.L., and Wolf, M., 1996, Schwertmannite and the chemical modeling of iron in acid sulfate waters: Geochimica et Cosmochimica Acta, v. 60, p. 2111–2121.

Bove, D.J., Mast, M.A., Wright, W.G., Verplanck, P.L., Meeker, G.P., and Yager, D.B., 2000, Geologic control on acidic and metal-rich waters in the southeast Red Mountains area, near Silverton, Colorado, *in* ICARD 2000; Proceedings of the Fifth International Conference on Acid Rock Drainage, Volume 1: Society for Mining, Metallurgy, and Exploration, Inc., p. 523–533.

Briggs, P.H., 1996, Forty elements by inductively coupled plasma–atomic emission spectroscopy, *in* Arbogast, B.F., ed., Analytical methods manual for the Mineral Resources Program, U.S. Geological Survey: U.S. Geological Survey Open-File Report 96–525, p. 77–94.

Burbank, W.S., and Luedke, R.G., 1969, Geology and ore deposits of the Eureka and adjoining districts San Juan Mountains, Colorado: U.S. Geological Survey Professional Paper 535, 73 p.

Burbank, W.S., Luedke, R.G., and Ward, F.N., 1972, Arsenic as an indicator element for mineralized volcanic pipes in the Red Mountains area, western San Juan Mountains, Colorado: U.S. Geological Survey Bulletin 1364, 31 p.

Carrara, P.E., Trimble, D.A., and Rubin, Meyer, 1991, Holocene treeline fluctuations in the northern San Juan Mountains, Colorado, U.S.A., as indicated by radiocarbon-dated conifer wood: Arctic and Alpine Research, v. 23, p. 233–246.

Casadevall, Thomas, and Ohmoto, Hiroshi, 1977, Sunnyside mine, Eureka mining district, San Juan County, Colorado—Geochemistry of gold and base metal ore deposition in a volcanic environment: Economic Geology, v. 72, p. 1285–1320.

Church, S.E., Fey, D.L., and Blair, Robert, 2000, Pre-mining bed sediment geochemical baseline in the Animas River watershed, southwestern Colorado, *in* ICARD 2000; Proceedings of the Fifth International Conference on Acid Rock Drainage, Volume 1: Society for Mining, Metallurgy, and Exploration, Inc., p. 499-512.

Comstock, T.B., 1883, Notes on the geology and mineralogy of San Juan County, Colorado: Transactions of the American Institute of Mining, Metallurgical and Petroleum Engineers, Inc., v. 11, p. 165–191.

Cross, C.W., Howe, Ernest, and Irving, J.D., 1905, Descriptions of the Silverton quadrangle: U.S. Geological Survey Atlas Folio 120, 20 p.

Cross, C.W., and Purington, C.W., 1899, Descriptions of the Telluride quadrangle: U.S. Geological Survey Atlas Folio 153, 19 p.

Elias, S.A., Carrara, P.E., Toolin, L.J., and Jull, A.J.T., 1991, Revised age of deglaciation of Lake Emma based on new radiocarbon and macrofossil analyses: Quaternary Research, v. 36, p. 307–321.

Fall, P.L., 1997, Timberline fluctuations and late Quaternary paleoclimates in the Southern Rocky Mountains, Colorado: Geological Society of America Bulletin, v. 109, p. 1306–1320.

Faure, Gunter, 1986, Principles of isotope geology, Second Edition: New York, John Wiley, 589 p.

Fisher, F.S., and Leedy, W.P., 1973, Geochemical characteristics of mineralized breccia pipes in the Red Mountain mining district, San Juan Mountains, Colorado: U.S. Geological Survey Bulletin 1381, 43 p.

Furniss, George, and Hinman, N.W., 1998, Ferricrete provides record of natural acid drainage, New World District, Montana, *in* Arehart, G.B., and Hulston, J.R., eds., 9th International symposium on water-rock interaction: Rotterdam, Balkema, p. 973–976.

Furniss, George, Hinman, N.W., Doyle, G.A., and Runnells, D.D., 1999, Radiocarbon-dated ferricrete provides a record of natural acid rock drainage and paleoclimatic changes: Environmental Geology, v. 37, p. 102–106.

Hanshaw, Bruce, 1974, Geochemical evolution of a goethite deposit, *in* 1st International symposium on water-rock interactions: Rotterdam, Balkema, p. 70–75.

Harrer, C.M., and Tesch, W.J., Jr., 1959, Reconnaissance of iron occurrences in Colorado: Bureau of Mines Information Circular 7918, 82 p.

Kirkham, R.M., Lovekin, J.R., and Sares, M.A., 1995, Sources of acidity and heavy metals in the Alamosa River basin outside of the Summitville mining area, Colorado, *in* Posey, H.H., Pendleton, J.A., and Van Zyl, D.J.A., eds., Proceedings; Summitville Forum '95: Colorado Geological Survey, p. 42–57.

Lamplugh, G.W., 1902, Calcrete: Geologic Magazine, v. 9, p. 575.

Logsdon, M.J., Miller, Scott, Swanson, Eric, Goodhard, William, and Perino, Larry, 1996, Pre-mining water quality in historically mined areas; iron bogs and ferricretes in the San Juan Mountains, Colorado: Geological Society of America Abstracts with Programs, v. 28, p. 518.

Luedke, R.G., 1975, Preliminary geologic map of the Silverton quadrangle, Colorado: U.S. Geological Survey Open-File Report 75–433, scale 1:20,000.

Luedke, R.G., and Burbank, W.S., 1987, Geologic map of the Handies Peak quadrangle, San Juan, Hinsdale, and Ouray counties, Colorado: U.S. Geological Survey Quadrangle Map GQ–1595, scale 1:24,000.

Mason, R.J., Brink, A.B., and Knight, K., 1959, Pleistocene climatic significance of calcretes and ferricretes: Nature, v. 184, no. 4685, p. 568.

Mast, M.A., Evans, J.B., Leib, K.J., and Wright, W.G., 2000, Hydrologic and water-quality data at selected sites in the upper Animas River watershed, southwestern Colorado, 1997–99: U.S. Geological Survey Open-File Report 00–53, 20 p.

Mast, M.A., Verplanck, P.L., Yager, D.B., Wright, W.G., and Bove, D.J., 2000, Natural sources of metals to surface waters in the upper Animas River watershed, Colorado, *in* ICARD 2000; Proceedings of the Fifth International Conference on Acid Rock Drainage, Volume 1: Society for Mining, Metallurgy, and Exploration, Inc., p. 513–522.

Miller, W.R., Bassett, R.L., McHugh, J.B., and Ficklin, W.H., 1999, The behavior of trace metals in water during natural acid sulfate weathering in an alpine watershed, *in* Filipek, L.H., and Plumlee, G.S., eds., The environmental geochemistry of mineral deposits—Part B, Case studies and research topics: Society of Economic Geologists, Reviews in Economic Geology, v. 6B, p. 492–503.

Nahon, D.B., 1991, Self-organization in chemical lateritic weathering: Geoderma, v. 51, p. 5–13.

Nash, J.T., 1999, Geochemical investigations and interim recommendations for priority abandoned mine sites, BLM lands, upper Animas River watershed, San Juan County, Colorado: U.S. Geological Survey Open-File Report 99–0323, 43 p.

Plumlee, G.S., Gray, J.E., Roeber, M.M., Jr., Coolbaugh, Mark, Flohr, Marta, and Whitney, Gene, 1995, The importance of geology in understanding and remediating environmental problems at Summitville, *in* Posey, H.H., Pendleton, J.A., and Van Zyl, D.J.A., eds., Proceedings; Summitville Forum '95: Colorado Geological Survey, p. 13–22.

Ransome, F.L., 1901, A report on the economic geology of the Silverton quadrangle, Colorado: U.S. Geological Survey Bulletin 182, 265 p.

Ringrose, C.R., 1982, Geology, geochemistry, and stable isotopes of a porphyry-style hydrothermal system, west Silverton district, San Juan Mountains, Colorado: Aberdeen, Scotland, University of Aberdeen Ph. D. dissertation, 256 p., 19 plates.

Stuiver, Minze, and Braziunas, T.F., 1993, Sun, ocean, climate and atmospheric $^{14}CO_2$; An evaluation of causal and spectral relationships: The Holocene, v. 3, p. 289–305.

Stuiver, Minze, and Reimer, P.J., 1993, Extended ^{14}C database and revised CALIB radiocarbon calibration program: Radiocarbon, v. 35, p. 215–230.

Stuiver, Minze, Reimer, P.J., Bard, E., Beck, J.W., Burr, G.S., Hughen, K.A., Kromer, B., McCormac, F.G., van der Plicht, J., and Spurk, M., 1998, INTCAL98 Radiocarbon age calibration 24,000–0 cal B.P.: Radiocarbon, v. 40, p. 1041–1083.

Vhay, J.S., 1962, Geology and mineral deposits of the area south of Telluride, Colorado: U.S. Geological Survey Bulletin 1112–G, p. 209–310.

Yager, D.B., Mast, M.A., Verplanck, P.L., Bove, D.J., Wright, W.G., and Hageman, P.L., 2000, Natural versus mining-related water quality degradation to tributaries draining Mount Moly, Silverton, Colorado, *in* ICARD 2000; Proceedings of the Fifth International Conference on Acid Rock Drainage, Volume 1: Society for Mining, Metallurgy, and Exploration, Inc., p. 535–550.